

A Radial-Flow Apparatus for Determining the Thermal Conductivity of Loose-Fill Insulations to High Temperatures

D. R. Flynn

(November 28, 1962)

A description is given of an apparatus used for determining the thermal conductivities of loose-fill granular materials in the temperature range 100 to 1,100 °C. The method used in making these determinations was that of radial heat flow through a hollow cylinder of specimen material contained between a central ceramic core and an outer ceramic shell. The heat flow through the specimen was determined by measurement of the power input to a heater in the central ceramic core. The radial temperature drop through the specimen was inferred from temperatures measured in the core and in the shell, thus avoiding entirely the problems of measuring a temperature difference within the specimen material. Experimental results with an estimated uncertainty of 3 percent or less are presented for diatomaceous earth having a density of 0.15 g/cm³, and for aluminum oxide powders having densities of 0.40 and 0.44 g/cm³. A discussion of the test method is given, with attention to possible sources of error.

1. Introduction

Various loose-fill thermal insulations are used, in conjunction with appropriate guarding, to reduce extraneous heat flows in several thermal conductivity measuring devices under development in the Heat Transfer Section at the National Bureau of Standards. Since such heat flows cannot be entirely eliminated, it is necessary to know the approximate thermal conductivity of these insulations in order to effect appropriate corrections. In designing an apparatus for determining the thermal conductivity of these insulations, it was decided to aim for an accuracy of 5 percent or better, because of the general interest in thermal conductivity of loose-fill materials, both from an engineering and from a theoretical viewpoint.

The purpose of this paper is to describe an apparatus and method used for determining the thermal conductivity of loose-fill materials. Experimental results are presented for diatomaceous earth and aluminum oxide powder in the temperature range from 100 to 1,100 °C. Factors affecting both the precision and accuracy of the measurements are discussed.

2. Method

Radial heat flow in a hollow cylinder of loose-fill insulating material was selected as the method for the measurements. A cross section of the essential elements of the apparatus is shown in figure 1. The specimen was contained within the annular space between the outer radius, a , of the ceramic core and the inner radius, b , of the concentric shell. A known quantity of heat per unit time generated electrically in the ceramic core flowed radially through the specimen to the concentric ceramic shell. The ceramic

core had a concentric ring of equally spaced holes at a radius, r' , parallel to the axis, each containing a heater wire. Temperatures were measured by an axial thermocouple in the ceramic core and by tangential thermocouples in the ceramic shell at radius c , only one of which is shown in figure 1.

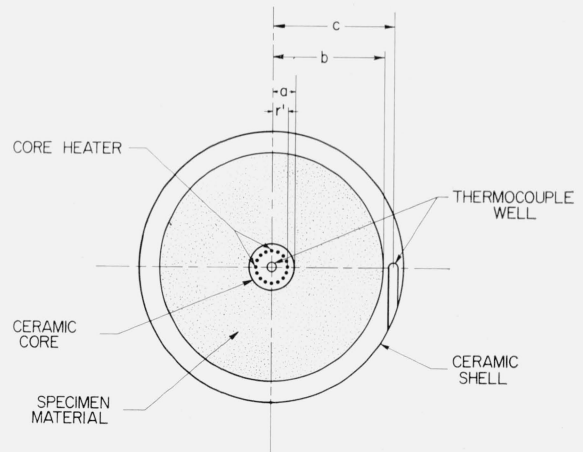


FIGURE 1. Horizontal cross section of the essential elements of the apparatus.

In figure 1, if the cylindrical surfaces $r=a$ and $r=b$ are each isothermal, the heat flow between these surfaces will be radial except near the ends. In general, the thermal conductivity of the specimen material will vary with temperature, and the heat flow rate, q , through a cylindrical element of unit axial length is

$$q = -2\pi kr \frac{dT}{dr} \quad (1)$$

Temperature is denoted by the symbol T , the temperature-dependent thermal conductivity by k , and the radial coordinate by r . For reasonable temperature differences, the thermal conductivity of the specimen material can be assumed to vary linearly with temperature; then (1) becomes

$$q = -2\pi\bar{k}\{1 + \alpha(T - \bar{T})\}r \frac{dT}{dr} \quad (2)$$

\bar{k} is the thermal conductivity at an arbitrary reference temperature, \bar{T} , and α is the corresponding temperature coefficient of thermal conductivity. Integration of (2) yields, after substitution of boundary conditions,

$$q = \frac{2\pi\bar{k}(T_a - T_b)}{\ln b/a}, \quad (3)$$

where T_a is the temperature at $r=a$, T_b is the temperature at $r=b$, and \bar{k} corresponds to the temperature \bar{T} , which is given by

$$\bar{T} = \frac{T_a + T_b}{2} \quad (4)$$

If the circle of heater wires at $r=r'$ were a continuous cylindrical heat source, the entire region $r < r'$ inside the heater circle would be isothermal. For the case of a finite number of line heat sources at $r=r'$, the temperature measured at the axis is equal to the average temperature at the radius of the heater circle [1]¹ (see also sec. 5). The heat flow to the surface of the core per unit length is given by

$$q = \frac{2\pi k_c(T_0 - T_a)}{\ln a/r'}, \quad (5)$$

where T_0 is the temperature measured in the axial well, and k_c is the thermal conductivity of the ceramic core material, corresponding to a temperature $(T_0 + T_a)/2$.

Similarly, for the outer ceramic shell,

$$q = \frac{2\pi k_s(T_b - T_c)}{\ln c/b}, \quad (6)$$

where T_c is the temperature measured at $r=c$, and k_s is the thermal conductivity of the ceramic shell material at $(T_b + T_c)/2$.

If there are m heater wires at $r=r'$, each generating heat at the rate q' per unit length, the total heat generated per unit length of core is

$$q = mq' \quad (7)$$

Combination of eqs (3), (5), (6), and (7) yields

$$\bar{k} = \frac{mq' \ln b/a}{2\pi \left\{ T_0 - T_c - \frac{mq'}{2\pi} \left(\frac{\ln a/r'}{k_c} + \frac{\ln c/b}{k_s} \right) \right\}}, \quad (8)$$

which is the equation used for purposes of calculation of all thermal conductivity data presented in this paper.

3. Experimental Procedure

3.1. Apparatus

A vertical cross section of the thermal conductivity apparatus is shown in figure 2. The specimen was contained in the annular space between the central ceramic core, which was supported at both ends, and the concentric ceramic shell, which was supported by Transite end pieces. The space between the ceramic shell and the outer stainless steel case contained a loose-fill thermal insulation.

The ceramic shell was a hollow mullite cylinder, 61 cm long, with an inner radius of 3.2 cm and an outer radius of 3.8 cm. A helical groove (about 1.6 turns/cm) on the outer surface was wound with three separate heaters of 0.10 cm Kanthal A-1 heater wire. The main shell heater was 41 cm in length; the upper and lower shell heaters were 5 cm in length. A length of 5 cm at each end was not wound. The upper and lower shell heaters provided extra heat needed to offset end losses, so that longitudinal temperature differences in the central region could be minimized.

The central core was an extruded mullite rod, 46 cm long and 1.27 cm in diameter. Sixteen equally spaced holes, 0.08 cm in diameter, extended the entire length of the rod. The centers of the holes formed a circle of 0.43 cm radius. The core heater, which provided the heat flowing radially through the specimen, consisted of a continuous length of platinum-20 percent rhodium (0.05 cm diam) wire threaded back and forth through the 16 holes. Current lead wires to this heater, and lead wires to its two voltage taps located at the upper end of the ceramic core, were brought in through the hollow ceramic upper support for the core. The core was supported below by a ceramic pin, as shown in figure 2. Both the upper and lower supports were provided with small platinum-20 percent rhodium heaters to minimize longitudinal heat flow at the ends of the ceramic core.

Temperatures in the apparatus were determined by means of six platinum: platinum-10 percent rhodium thermocouples. These thermocouples were fabricated from calibrated thermocouple wire, 0.04 cm in diameter.

Three thermocouples were positioned in the ceramic shell at the midplane of the apparatus. These were inserted into tangential holes (fig. 1) located 120° apart at a radius of 3.5 cm. The temperature, T_c , in (6) and (8) was obtained by taking the average of the temperatures indicated by these three thermocouples. Two additional tangential thermocouples were located in the ceramic shell, one 15 cm above and one 15 cm below the midplane of the apparatus.

Temperatures in the core were measured by means of a thermocouple which was located in a 0.25-cm diam axial well and which could be moved vertically

¹ Figures in brackets indicate the literature references at the end of this paper.

by exterior manipulation. A scale fixed above the apparatus indicated the position of the thermocouple junction. The temperature measured at midlength was designated as T_0 .

3.2. Instrumentation

The three heaters on the ceramic shell were fed by variable voltage transformers, which in turn were fed by a voltage regulating transformer. These heaters were individually regulated by on-off controllers actuated by thermocouples located in the ceramic shell adjacent to the heater windings. The heaters on the ceramic core supports were manually adjusted by means of variable voltage transformers.

The ceramic core heater, which provided the heat flowing radially through the specimen, was powered by a 28-v, 4-amp, regulated d-c power supply, with a small bank of power resistors in series for adjusting to the desired heater current. Power input to the ceramic core heater was determined by measuring the d-c current through the heater and the voltage drop across the entire length of heater wire in the core. These measurements were made using calibrated shunt and volt boxes and measuring their output voltages by means of a precision d-c potentiometer.

The noble metal leads of the six measuring thermocouples were brought to an isothermal zone box at room temperature. A thermocouple with one junction in the zone box and one in an ice bath was placed in series with a double-pole selector switch, so that each measuring thermocouple was automatically referenced against the ice bath [2]. Thermocouple voltages were read to 0.1 μV on the precision potentiometer.

3.3. Test Procedure

The specimen material was placed in the annular space between the ceramic core and the ceramic shell through the opening at the top of the apparatus. The bulk density of the specimen in place was computed from the weight of specimen material and the volume of the test chamber.

The shell temperature controllers were set at the desired temperature, which for the first test in any series was about 100 °C, and all heaters were turned on. The controllers and power for the heaters at the top and bottom of the ceramic shell were adjusted, if necessary, until the temperatures indicated by the upper and lower tangential thermocouples agreed to within 1 or 2 deg C with the average temperature of the three midplane tangential thermocouples. The power to the core heater was adjusted to attain the desired radial temperature drop across the specimen, and the power to the heaters on the ceramic core supports was adjusted until a traverse of the thermocouple in the axial hole indicated the desired longitudinal temperature distribution.

When a satisfactory steady-state condition was obtained, the test data were recorded. With the axial thermocouple in the midplane position, three sets of readings (at about 20 min intervals) were

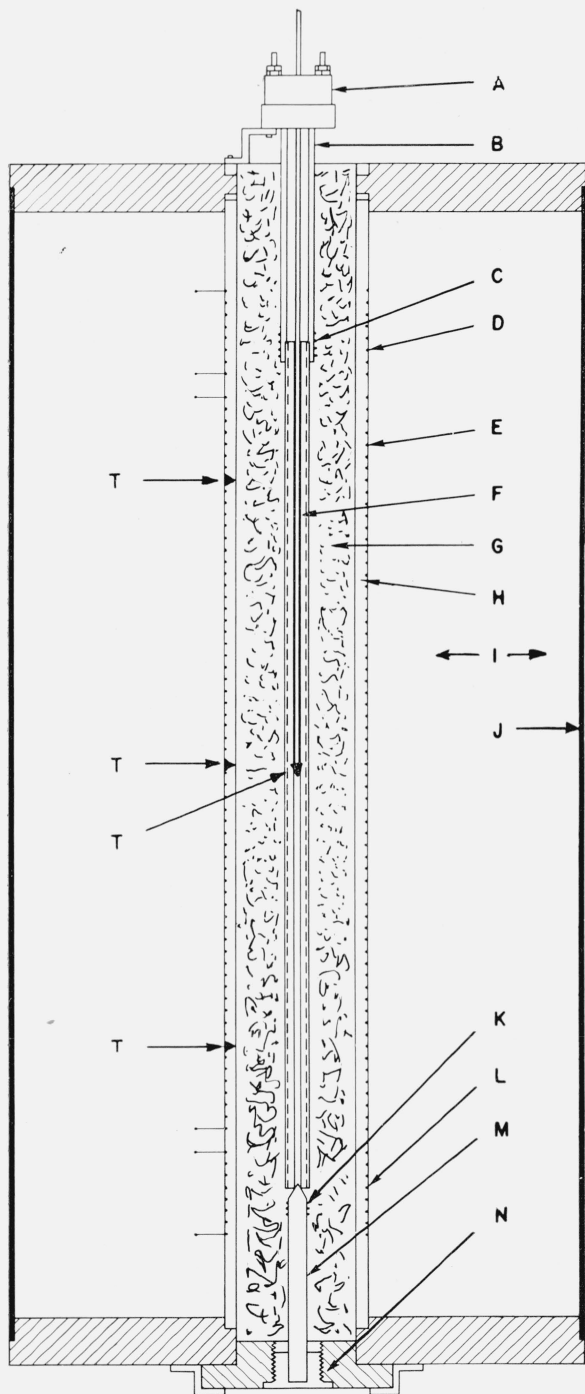


FIGURE 2. Vertical cross section of the apparatus for determining the thermal conductivity of powders.

- | | |
|---|--------------------------|
| A. Terminal head for current and voltage leads. | H. Ceramic shell. |
| B. Ceramic support tube. | I. Shell insulation. |
| C. Upper support heater. | J. Stainless steel case. |
| D. Upper shell heater. | K. Lower support heater. |
| E. Main shell heater. | L. Lower shell heater. |
| F. Ceramic core. | M. Ceramic support rod. |
| G. Specimen. | N. Removable plug. |
| | T. Thermocouple. |

taken of all thermocouples and of the output of the volt box and shunt box. At the end of these readings, the axial thermocouple was moved to a position near the top of the ceramic core. After this thermocouple again reached thermal equilibrium, its output was read on the potentiometer. Readings were taken at 5 cm intervals over a region 15 cm or more on either side of the midplane. When a complete set of data had been taken, the apparatus was adjusted to a new temperature level, as desired for the next test.

3.4. Calculation of Results

Calculations of thermal conductivity values by means of eq (8) were performed by means of a digital computer. The data input to the computer consisted of the average emf readings for each thermocouple and the average readings from the volt and shunt boxes. Equations for the estimated thermal conductivities of the ceramic core and shell as functions of temperature, and for temperatures as a function of thermocouple emfs, were contained in the computer program.

4. Results

4.1. Diatomaceous Earth

Test results for a specimen of commercial diatomaceous earth are presented in figure 3. The in-place bulk density of the specimen was 0.15 g/cm³. The temperature difference across the specimen during the various tests was from 30 to 60 deg C.

The open squares in figure 3 represent results obtained in five tests before heaters were placed at the ends of the ceramic core to minimize axial heat flows. For these five tests, the temperature differ-

ence between the ceramic core and shell was 10 to 25 percent less at positions 15 cm from the midplane than it was at the midplane. (These data, as well as those presented below, were calculated using eq (8); the effect of a nonuniform axial temperature distribution is discussed in sec. 5.2.)

After these five tests, the specimen was removed and heaters were installed on the ceramic core supports. The same sample was then reinstalled as the specimen, and the data represented by the open circles were taken in order of increasing mean temperature. After the test at a mean temperature of 946 °C, tests were conducted at several lower temperatures and finally at a maximum temperature. The results of these tests, indicated in figure 3 by circles with vertical lines through them, were significantly higher than those of previous tests. Removal of the specimen indicated that a slight sintering had occurred.² The powder appeared to be slightly fused together, but was easily broken apart. The same sample was pulverized by hand, replaced in the apparatus, and the test results indicated by the open triangles were obtained.

The curve drawn through the data points in figure 3 is the quadratic equation of least-mean-squares fit to the open squares, circles, and triangles. The equation for this line is

$$\bar{k} = 0.414 + 1.114 \left(\frac{\bar{T}}{1000} \right) + 0.072 \left(\frac{\bar{T}}{1000} \right)^2, \quad (9)$$

where \bar{k} is expressed in milliwatts/cm-deg C and \bar{T} in °C. For all data points except the circles with vertical lines through them, the standard deviation of a point, estimated from the residuals about the fitted line, is 0.013 mw/cm-C, corresponding to 1.3 percent at 500 °C.

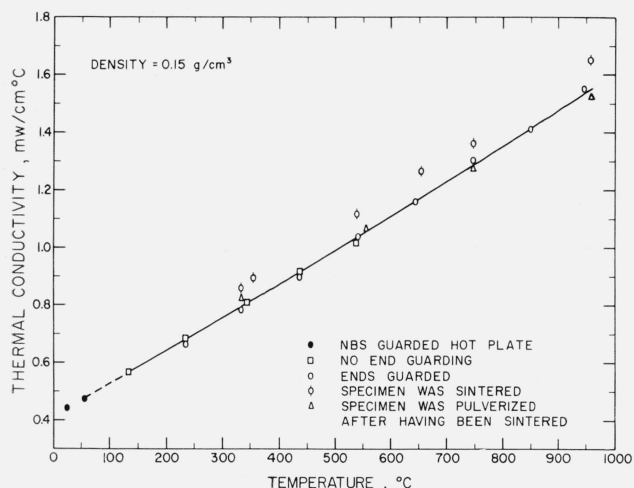
The solid circles shown in the lower left hand corner of figure 3 represent results of tests made on a sample of diatomaceous earth from the same container, at the same density, in the NBS guarded hot-plate apparatus (ASTM C177).

Figure 4 presents some literature data on diatomaceous earth of various densities [3, 4]; the curve from figure 3 is reproduced for comparison. There is substantial agreement between the results of this investigation and those from the literature, taking density into consideration.

4.2. Powdered Alumina

Test results for an aluminum oxide powder are presented in figure 5. This alumina was produced at the National Bureau of Standards by ignition of hydrated aluminum chloride in a muffle furnace at 1,150 °C. The method of production and some of the properties of this type of alumina powder have been described [5].

² An uncontaminated diatomaceous earth should melt at the temperature of fusion of silica, which is well above any temperatures obtained in these tests. A commercial diatomaceous earth, however, may contain sufficient clay to produce sintering at temperatures as low as 800 °C. No tests were conducted to determine the actual temperature at which sintering began for the diatomaceous earth discussed in this paper. In general, diatomaceous earth should be used with caution at temperatures above 800 °C if sintering would cause difficulties.



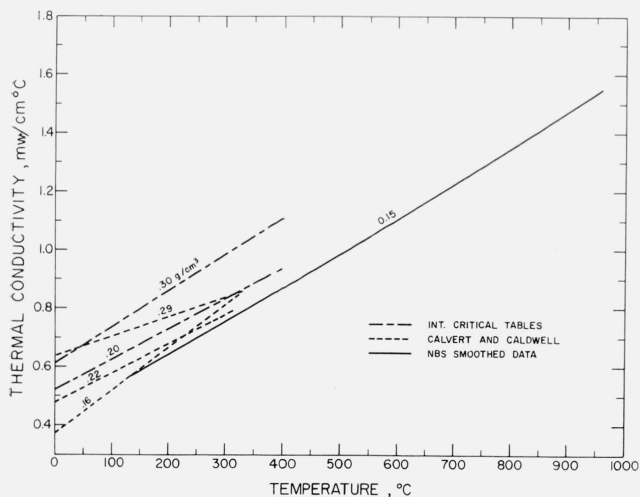


FIGURE 4. Comparison of diatomaceous earth thermal conductivity results with literature data.

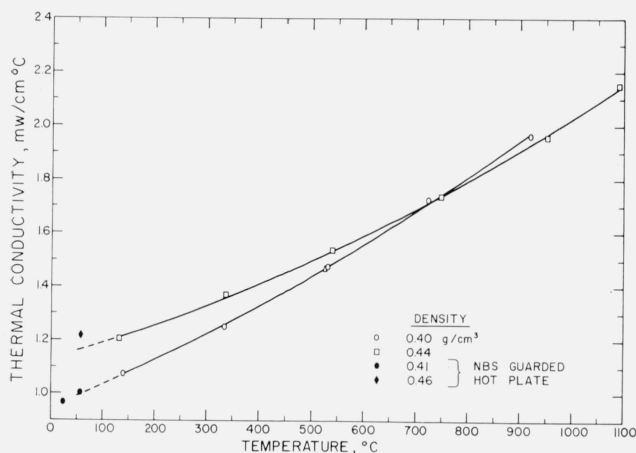


FIGURE 5. Thermal conductivity of an aluminum oxide powder as a function of temperature.

The data indicated by the open squares in figure 5 were taken in order of increasing mean temperature on a specimen having a bulk density³ of 0.44 g/cm³. The curve drawn through the squares is the quadratic equation of least-mean-squares fit. The equation for this line is

$$\bar{k} = 1.130 + 0.566 \left(\frac{\bar{T}}{1000} \right) + 0.333 \left(\frac{\bar{T}}{1000} \right)^2, \quad (10)$$

where \bar{k} is expressed in mw/cm-C and \bar{T} in °C. The estimated standard deviation of a point is 0.010 mw/cm-C, corresponding to 0.7 percent at 500 °C.

³ Later checks of the packing procedure used for this specimen indicate a possible uncertainty of 0.02 g/cm³ in the reported in-place bulk density. All other densities reported are believed to be accurate to within 0.005 g/cm³.

The data indicated by the open circles were taken in order of increasing mean temperature on a specimen having a bulk density of 0.40 g/cm³. The specimen was the same sample as that previously tested, but was intentionally packed to a lower bulk density. After the tests up to 919 °C, a test, indicated by an open triangle, was made at 526 °C. The curve drawn through the open circles and the triangle is the quadratic equation of least-mean-squares fit to these points. This equation is

$$\bar{k} = 0.947 + 0.841 \left(\frac{\bar{T}}{1000} \right) + 0.296 \left(\frac{\bar{T}}{1000} \right)^2, \quad (11)$$

in the same units as above. The estimated standard deviation of a point is 0.011 mw/cm-C, corresponding to 0.8 percent at 500 °C.

The solid circles shown in the lower left-hand corner of figure 5 represent results of two tests made in the NBS guarded hot-plate apparatus on a sample of alumina powder, taken from the same batch as the sample installed in the ceramic core apparatus, having a bulk density of 0.41 g/cm³. The solid diamond shown represents a guarded hot-plate test on the sample of alumina which had been tested in the ceramic core apparatus at higher temperatures. The in-place bulk density for this test was 0.46 g/cm³.

The higher density specimen (0.44 g/cm³) had a room temperature thermal conductivity about 20 percent higher than that of the lower density specimen (0.40 g/cm³). However, the curves corresponding to these different densities converged with increasing temperature and crossed at about 730 °C. This crossing of the curves is believed to arise from increased radiation within the larger pores of the lower density material.

5. Discussion of Test Method

5.1. Determination of Temperature Difference Across the Specimen

Measurement of the temperature difference across the specimen, using the core and shell thermocouples shown in figure 1, represents a departure from the procedure used in radial flow methods for loose-fill materials described in the recent literature [6, 7]. The possibility of chemical contamination of thermocouples by the specimen material is greatly reduced, and the often-difficult problem of determining and maintaining the distance between thermocouples located within the specimen material is avoided. However, with the method of measurement used here, account must be taken of temperature drops in the core and shell, and at their interfaces with the specimen if necessary, to obtain the temperature drop across the specimen.

The thermocouple in the axial hole at midlength of the central ceramic core is located in a region where there are substantially no temperature gradients, and therefore the thermocouple accurately attains the temperature of its environment without disturbing the heat flow pattern. The theory of a harmonic logarithmic potential function shows that

the value of the temperature at the center of a circle is equal to the average of its values over the circumference of the circle [8,9]. Hence, the temperature measured at the axis of the core is equal to the average temperature at the fictitious surface, $r=r'$. The difference between the average temperature of the fictitious surface at $r=r'$ and the average temperature of the surface of the core at $r=a$ may be computed from (5). It is to be noted that eq (5) is valid regardless of the distribution of heat sources on the circle $r=r'$, as has also been shown by Peavy [1] in analyzing the two-body system of the specimen and the core with line heat sources.

Similarly, the temperature difference, $T_b - T_c$, from the inner surface of the shell to the radius of the tangential thermocouples may be computed from (6).

The uncertainty in determining the temperature difference between the axial thermocouple in the core and the three thermocouples in the shell is estimated⁴ to be less than 1 percent. The computed temperature drops in the core ($T_0 - T_a$) and in the shell ($T_b - T_c$) were less than 2.4 percent and 0.6 percent, respectively, of the temperature drop through the specimen for all of the results presented in section 4, using the best available values for the thermal conductivities of the mullite core and shell, the uncertainties in which may have been as much as 30 percent.

The effective radius, r' , of the virtual heating surface in the core is uncertain by not more than the radius of the heater holes, thus introducing an additional error of not more than 25 percent of $T_0 - T_a$. Similarly, the effective radius, c , to the tangential thermocouple wells is uncertain by not more than the radius of the wells, thus introducing an additional error of not more than 35 percent of $T_b - T_c$. Combining the errors arising from the uncertainties in k_c and k_s and those from $\ln a/r'$ and $\ln c/b$, the estimated uncertainties in $T_0 - T_a$ and $T_b - T_c$ are 40 and 50 percent, respectively, thus introducing an additional uncertainty in $T_a - T_b$ of 1.3 percent. For fine powders of low thermal conductivity, such as those tested, errors due to thermal contact resistance between the specimen and the surfaces of the core and shell are believed to be negligible. Thus, combining uncertainties, the temperature drop across the specimen (the expression in braces in the denominator of eq (8)) is considered to be known with an uncertainty of 1.5 percent.

5.2. Longitudinal Heat Flow

Equation (8) was derived on the assumption of no longitudinal heat flow. For an apparatus of finite length, having imperfect end guarding, the effects of axial heat flow should be considered. Jakob [11] considered the effect of axial heat flow for the symmetrical case in which both ends of the core are at the same temperature but are at a temperature different from that at the center. An analysis is presented here which allows different temperatures

⁴ All estimated uncertainties in this paper represent the author's estimate of the "two-sigma" limit. All uncertainties are combined using standard propagation of error formulas (see, for instance, Davies [10]).

at the two ends of the core, and also takes into account the effect of core temperature distribution on the power measurement if the electrical resistivity of the heater wire varies linearly with temperature.

A simplified cross-sectional view of the apparatus is shown in figure 6. It is assumed that the surface $r=b$ is isothermal at temperature T_b and that temperatures are measured in the core at three positions equally spaced along the axis. It is assumed that, for the purpose of analyzing longitudinal heat flow, a transverse cross section of the core can be treated as being isothermal.

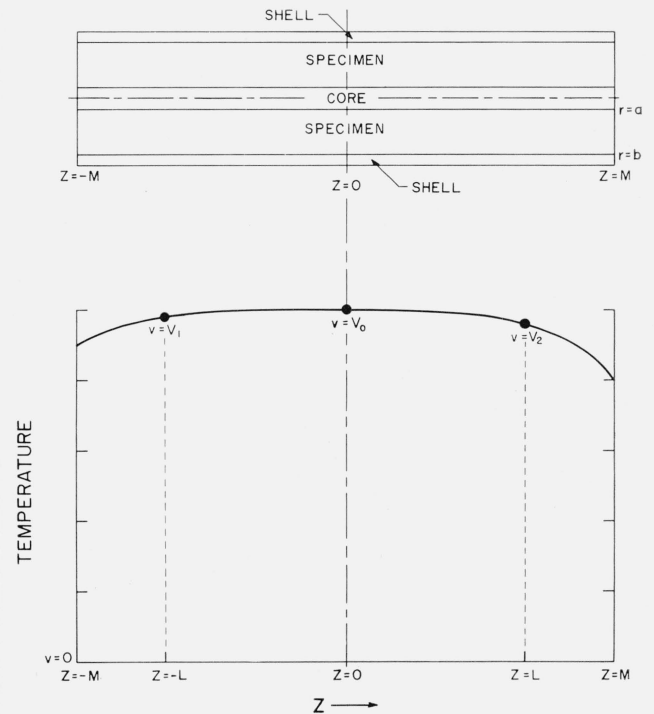


FIGURE 6. General core temperature profile used in analyzing effects of longitudinal core temperature imbalance.

Neglecting longitudinal heat flow in the specimen, the differential equation for heat flow along the core can be written as

$$\frac{d^2 v}{dz^2} - \frac{2\pi \bar{k} v}{C \ln b/a} = -\frac{mq'}{C}, \quad (12)$$

where

$v = T - T_b$, T being the temperature at any point along the core;
 z = longitudinal coordinate;

and

C = the longitudinal thermal conductance per unit length of the core, including heater wires and holes.

In general, the rate of heat generation, q' , per unit length of heater wire will not be constant if the electrical resistivity of the heater wire varies appreciably

with temperature. For reasonable temperature variations, the electrical resistance per unit length of heater wire can be assumed to be a linear function of temperature,

$$\rho = \rho_0(1 + \gamma v), \quad (13)$$

where ρ and ρ_0 are the electrical resistances of a unit length of heater wire at temperatures T and T_0 , respectively, and γ is the fractional change in electrical resistivity per unit change in temperature. The rate of heat generation per unit length of heater wire is

$$q' = I^2 \rho = I^2 \rho_0(1 + \gamma v), \quad (14)$$

where I is the electrical current flowing through the heater. Equation (14) must be substituted into (12).

The conditions which are to be satisfied are

$$\begin{aligned} v &= V_1 \text{ at } z = -L, \\ v &= V_0 \text{ at } z = 0 \\ v &= V_2 \text{ at } z = L \end{aligned} \quad (15)$$

Substitution of these conditions into the solution of (12) yields

$$\begin{aligned} v = V_0 + \left(\frac{V_1 + V_2 - 2V_0}{2} \right) \frac{\cosh \mu z - 1}{\cosh \mu L - 1} \\ + \left(\frac{V_2 - V_1}{2} \right) \frac{\sinh \mu z}{\sinh \mu L}, \end{aligned} \quad (16)$$

in which

$$\mu^2 = \frac{1}{C} \left[\frac{2\pi \bar{k}}{\ln(b/a)} - \gamma m I^2 \rho_0 \right]. \quad (17)$$

The thermal conductivity of the specimen is given by

$$\bar{k} = \frac{m I^2 \rho_0 \ln(b/a)}{2\pi V_0} \left[1 + \gamma V_0 + \frac{V_1 + V_2 - 2V_0}{2V_0 \cosh \mu L - (V_1 + V_2)} \right]. \quad (18)$$

The total power delivered by the core heater is determined by the current, I , through the heater and the voltage drop, E , across the total length of heater wire in the core. The total resistance of the heater is given by

$$R = E/I = \rho_0(1 + \gamma \bar{V})S \quad (19)$$

where S is the total length of heater wire and \bar{V} is the average temperature of the core heater, obtained by integration of (16) over the entire length, $2M$, of the core,

$$\begin{aligned} \bar{V} = \frac{1}{2M} \int_{-M}^M v dz = V_0 \\ + \left(\frac{V_1 + V_2 - 2V_0}{2} \right) \frac{\sinh \mu M}{\mu M (\cosh \mu L - 1)}. \end{aligned} \quad (20)$$

Equation (18) can be rewritten as

$$\bar{k} = \bar{k}' \left[1 + \frac{V_1 + V_2 - 2V_0}{1 + \gamma \bar{V}} \left\{ \frac{1}{2V_0 \cosh \mu L - (V_1 + V_2)} - \frac{\gamma (\sinh \mu M - \mu M)}{2\mu M (\cosh \mu L - 1)} \right\} \right] \quad (21)$$

where

$$\bar{k}' = \frac{mEI \ln(b/a)}{2\pi V_0 S} \quad (22)$$

is the apparent value of thermal conductivity obtained if no corrections are made for the effects of axial heat flow. Since \bar{k} is defined in terms of μ and μ in terms of \bar{k} , iterations are necessary in order to obtain \bar{k} . A first approximation to \bar{k} is given by \bar{k}' ; substitution of \bar{k}' into (17) yields a value of μ which can be used in (21). The resultant \bar{k} can be used to obtain a better value of μ , etc. The convergence is quite rapid in all practical cases; the first approximation did not introduce an inaccuracy greater than 0.003 percent in \bar{k} for the case to be discussed below. Equation (22) corresponds to (8), the equation that was used for purposes of calculation; EI/S corresponds to q' , and V_0 corresponds to the expression in braces in the denominator of (8). The first expression in the braces in (21) represents the correction for axial heat flow; the second expression represents the correction in power measurement to take account of the variation of electrical resistance with temperature. It is of interest to note that, for a positive value of γ , these corrections are of opposite sign.

Data were presented in section 4.1 for which the temperature difference between the ceramic core and the substantially isothermal ceramic shell was 10 to 25 percent less at positions 15 cm from the midplane than at the center. As seen in figure 3, the results for these tests were not appreciably different from the conductivities obtained later when the core was substantially uniform in temperature along its length.

In order to investigate more thoroughly the effects of axial heat flow in the apparatus, a series of five tests was conducted in which the ends of the ceramic core were held at temperatures different from that in the core at the midplane. These tests were all conducted at a mean temperature of 525 °C, with the alumina powder specimen discussed in section 4.2.

The ceramic shell was maintained approximately isothermal over a central region of at least 30 cm length. The core temperature at positions 15 cm above and below the midplane was varied by adjustment of the small heaters at each end of the ceramic core. The results of these tests are shown in figure 7, where the percent departure of the thermal conductivities from their mean value is plotted against the quantity $(V_1 + V_2)/2V_0$. The solid circles represent experimental data; the solid curve is the straight line of least-mean-squares fit to the data. A straight line was used because, for the various values of parameters involved, the departure can be shown to be a nearly linear function of $(V_1 + V_2)/2V_0$ for values

not too different from 1.0. The slope of the straight line in figure 7 was used to compute the value for μ of 0.29 cm^{-1} where γ was taken as $8.0 \times 10^{-4} \text{ deg C}^{-1}$, V_0 as 44 deg C , L as 15 cm , and M as 23 cm . Substitution of this value of μ into (17) yields for the longitudinal conductance of the core, \bar{C} , a value of 0.06 w-cm/C . This value agrees with the estimated longitudinal conductance of the ceramic core and heater wires.

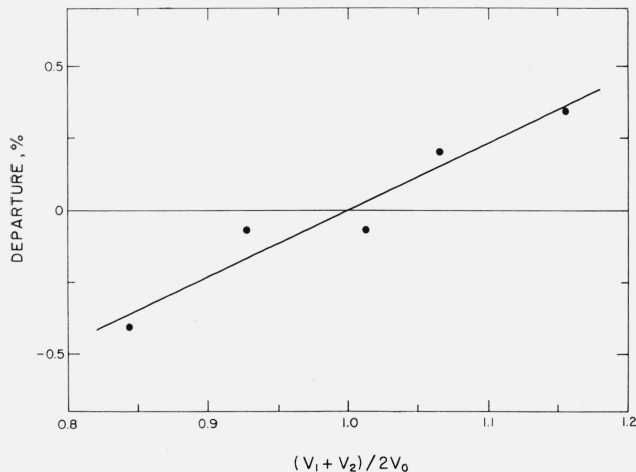


FIGURE 7. Effect of longitudinal core temperature imbalance, $(V_1 + V_2)/2V_0$, on thermal conductivity values obtained for alumina powder.

With the exception of those tests in which core end heaters were not used, all data presented in section 4 gave values of $(V_1 + V_2)/2V_0$ between 0.85 and 1.15. From figure 7, it is seen that this corresponds to an uncertainty of less than 0.4 percent in the thermal conductivity values obtained using (8). Values of $(V_1 + V_2)/2V_0$ could be held between 0.95 and 1.05 without undue difficulty, if desired, thus further reducing this uncertainty.

5.3. Eccentricity

It has been assumed that the outer surface of the ceramic core and the inner surface of the ceramic shell were concentric cylinders. Since concentricity may not always be possible, the effect of eccentricities should be considered. The thermal resistance between two eccentric parallel circular cylinders is given by Carslaw and Jaeger [12] and is, in the notation of this paper,

$$\frac{T_a - T_b}{q} = \frac{1}{2\pi\bar{k}} \operatorname{arccosh} \frac{a^2 + b^2 - e^2}{2ab}, \quad (23)$$

where e is the eccentricity, or the distance between the centers of the two cylinders.

From (23), the thermal conductivity is given by

$$\bar{k} = \frac{q}{2\pi(T_a - T_b)} \operatorname{arccosh} \frac{1 + \lambda^2 - \epsilon^2(\lambda - 1)^2}{2\lambda}, \quad (24)$$

where, following El-Saden [13], the dimensionless eccentricity $\epsilon = e/(b - a)$ varies between zero (concentricity) and one (cylinders in contact), and $\lambda = b/a$ is the ratio of the radii.^{5,6}

For the case of eccentric cylinders, if (3) is used instead of (24) to compute the thermal conductivity of the specimen, an error will be introduced. Since it is of general interest, the percent error due to neglecting the effect of eccentricity is shown in figure 8 plotted against dimensionless eccentricity, ϵ , for several radius ratios, $\lambda = b/a$.

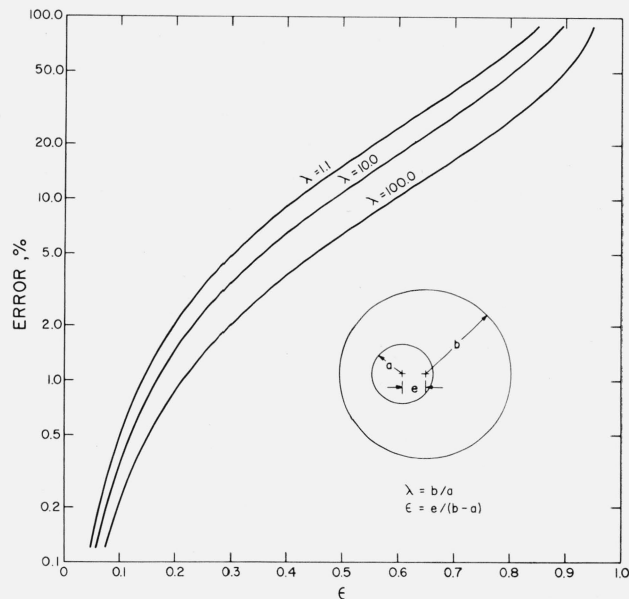


FIGURE 8. Calculated error in thermal conductivity due to neglecting the effect of eccentricity for radial heat flow between isothermal cylinders.

For the apparatus described in this paper, the ratio λ was approximately 5.0. The dimensionless eccentricity as defined above was less than 0.05, so that the uncertainty due to eccentricity was less than 0.1 percent.

5.5. Precision and Accuracy of Results

The precision of measurement is indicated by the standard deviations (estimated) of the data, which are of the order of 1 percent.

The accuracy of the reported measurements is more difficult to estimate. The total power generated in the core heater was known to within 0.1 percent. The length of wire between the potential taps at room temperature was known to within 0.2 percent. Thermal expansion could have increased this length by 1 percent at $1,000 \text{ }^\circ\text{C}$ if friction between the heater wire and the ceramic core at points of contact did not prevent free longitudinal expansion of the wire in the holes. Because the

⁵ Equation (24) can also be derived from the last equation presented by El-Saden. To convert El-Saden's eq (38) to the form presented above, it is helpful to make use of the identity $\operatorname{arccosh} x - \operatorname{arccosh} y = \operatorname{arccosh} (xy - \sqrt{(x^2 - 1)(y^2 - 1)})$.

⁶ Making use of the identity $\operatorname{arccosh} x = \ln(x + \sqrt{x^2 - 1})$, eq (24) reduces to the equivalent of (3) for the case of concentric cylinders ($\epsilon = 0$).

effect of expansion was uncertain, no expansion corrections were made. The heat flowing radially through the specimen is further in question by not more than 0.4 percent in an extreme case, due to the uncorrected effects of longitudinal temperature variations along the core (see sec. 5.2).

In section 5.1, it was estimated that temperature drops across the specimen were determined with an uncertainty of 1.5 percent. Uncertainties in the ratio of the shell radius to that of the core did not introduce more than 0.2 percent uncertainty in the results. The error due to possible eccentricity of the ceramic core in the ceramic shell did not exceed 0.1 percent. Combining all of the uncertainties discussed, uncertainties in the thermal conductivity results presented in section 4 are estimated to be less than 2 percent at 100 °C, and, because of heater wire expansion, 3 percent at 1,000 °C.

5.5. Comments

It is felt that the type of central heater used in this apparatus has advantages which may recommend it to others interested in radial heat flow measurements. The particular advantages of this arrangement are, (1) the measuring thermocouple in the core attains the temperature to be measured and does not interfere with the pattern of heat flow, (2) the measuring thermocouple is well protected both mechanically and chemically but still can be easily removed for calibration or renewal, and (3) temperatures can be measured at any desired longitudinal position using the same thermocouple.

By means of suitable modifications, the equipment described could be extended to cryogenic temperatures, or to more elevated temperatures. If required, the accuracy of measurement could be improved over that attained in the apparatus described by taking careful account of all the factors discussed in sections 5.1 and 5.2. Applications for which a heated core of this type might be advantageous include determination of forced or natural convection from cylinders and determination of the thermal conductivity of pipe insulations or fluids. In the latter case, convective effects would need to be excluded by extrapolating results obtained with small temperature differences to zero temperature difference.

The experimental measurements were performed by C. I. Siu and J. E. Griffith. The author thanks T. W. Watson for conducting the various tests on the NBS guarded hot plate apparatus. The very helpful suggestions and comments by B. A. Peavy and H. E. Robinson are gratefully acknowledged.

6. References

- [1] B. A. Peavy, Steady state heat conduction in cylinders with multiple continuous line heat sources, *J. Research NBS* **67C** (Eng. and Instr.) No. 2, 119-127 (Apr.-June 1963).
- [2] W. F. Roeser, Thermoelectric thermometry, *J. Appl. Phys.* **11**, pp. 404-405 (1940); also in *Temperature, Its Measurement and Control in Science and Industry*, p. 202 (Reinhold Publishing Corp., New York, N. Y., 1941).
- [3] *International Critical Tables*, Vol. II, p. 315 (McGraw-Hill, New York, N.Y., 1927).
- [4] R. Calvert and L. Caldwell, Loss of heat from furnace walls, *Ind. Eng. Chem.* **16**, pp. 483-490 (1924).
- [5] J. I. Hoffman, R. F. Leslie, H. J. Caul, L. J. Clark and J. D. Hoffman, Development of a hydrochloric acid process for the production of alumina from clay, *J. Research NBS* **37**, p. 409 (1946) RP1756.
- [6] R. G. Deissler and D. S. Eian, Investigation of effective thermal conductivities of powders, National Advisory Committee for Aeronautics RM E52C05 (1952).
- [7] M. J. Laubitz, Thermal conductivity of powders, *Can. J. Phys.* **37**, p. 798 (1959).
- [8] O. D. Kellogg, *Foundations of Potential Theory*, p. 223 (Frederick Ungar Publishing Co., New York, N. Y., 1929; reprinted by Dover Publications, Inc., New York, N. Y., 1953).
- [9] W. J. Sternberg and F. I. Smith, *The Theory of Potential and Spherical Harmonics*, pp. 74-76 (The Univ. of Toronto Press, Toronto, Canada, 1946).
- [10] O. L. Davies, *Statistical Method in Research and Production*, 3d ed., pp. 40-41 (Hafner Publ. Co., New York, N. Y., 1957).
- [11] M. Jakob, *Heat Transfer*, Vol. 1, pp. 246-250 (John Wiley and Sons, Inc., New York, N. Y., 1949).
- [12] H. S. Carslaw and J. C. Jaeger, *The Conduction of Heat in Solids*, 2d ed., p. 451, equation 19 (Oxford Univ. Press, 1959).
- [13] M. R. El-Saden, Heat conduction in an eccentrically hollow, infinitely long cylinder with internal heat generation, *J. Heat Transfer*, *Trans. ASME*, Series C, **83**, 510 (1961).

(Paper 67C2-126)